

Evaluating Human Behavior in Manual and Shared Control via Inverse Optimization

Jairo Inga, Michael Eitel, Michael Flad, Sören Hohmann

Institute of Control Systems (IRS)
Karlsruhe Institute of Technology (KIT)
Karlsruhe, Germany
jairo.inga@kit.edu

Abstract—Shared control systems have a great potential to contribute to a safer human-machine interaction. A great body of literature has been concerned with the design of the automation the human is sharing control with. At the same time, an adequate design is connected to the availability of reliable models of human behavior. A promising modeling approach is given by optimal control theory, where human behavior arises from the minimization of a cost function. However, most of the work found in literature focus on determining the cost function of the human in a situation without any haptic interaction with a partner, i.e. in manual control tasks. Motivated by several studies which indicate that human behavior changes when completing a task cooperatively, this paper proposes an optimal control approach for human behavior modeling in a shared control scenario. We further hypothesize that the human cost functions in a shared control scenario change significantly when compared to the ones which arise from a human performing a control task alone. We apply an inverse optimization approach in order to identify the cost function in both scenarios. In order to evaluate our hypothesis, a study was conducted where 42 participants performed a tracking task in a manual mode and then sharing control with an assistance system. The findings show that the model is able to describe human behavior in both shared and manual control. Furthermore, the results confirm that the human cost function changes considerably between both scenarios.

Index Terms—Shared Control, Human Behavior Identification, Inverse Optimal Control, Inverse Reinforcement Learning.

I. INTRODUCTION

The rising development of automated systems entails several challenges concerning human-machine interaction. One example is given by the so called ironies of automation [1], which state that humans are still required as a fallback solution in the case of system failures but do not have the situation awareness such a critical scenario demands. This problem can be addressed by keeping the human “in the control loop”, leading to the concept of haptic shared control where human and an automatic controller simultaneously interact with a dynamic system. This concept has received considerable attention and has been shown to lead to better overall performance with reduced control effort [2], better reaction times in a driving task [3] and lower cognitive workload [4]. It has also been successfully applied in several application fields. We mention here exemplarily robot-aided rehabilitation [5], surgical systems [6], advanced driver assistance systems [7] and teleoperation of unmanned aerial vehicles [8].

In the shared control scenario, the human behavior model plays a fundamental role, since it provides a useful asset for the adaption of the automation to the human. Several studies have indicated the potential of a human behavior model to improve shared control systems [9]–[11]. The benefits of such a model include not only a higher user acceptance, but also a safer and more effective interaction due to a better agreement between control actions. This follows as a consequence of being able of predicting human behavior.

A modeling approach which is receiving considerable attention is the use of optimality principles and dynamic optimization in form of optimal control [12]–[15]. The theory states that human motion arises from the optimization of a cost function, a process which is believed to take place in the central nervous system [16]. In this context, the aim is to recover a cost function with respect to which the observed human control trajectories are optimal. Mathematically speaking, this is known as the *inverse optimal control* problem. Many methods have been proposed for its solution. Most of them give the cost function a particular structure which reduces the problem to the identification of cost function parameters. We mention here exemplarily direct approaches [17], methods based on optimality conditions [18] and inverse reinforcement learning techniques which stem from computer science [19].

While these approaches have been shown to be able to model and identify human behavior adequately, they have so far only been developed for human behavior without any interaction with a partner. Moreover, several studies indicate that human behavior when performing a task in a cooperative scenario is not the same as when performing it alone [2], [20], [21]. Thus, it is questionable whether these models are able to describe human behavior in a shared control task, as they do not consider the interaction with a cooperating partner. If the model fails to account for this differences, stability issues and even hazardous behavior of the machine can potentially arise as a consequence of model mismatch. It is crucial to develop a model which is able to describe these differences.

Therefore, in this paper, we present an optimal control approach for modeling human behavior where the influence of the machine is taken into account. We assess the question whether the cost function parameters change when performing a control task cooperatively and manually. Furthermore, we analyze if the presented optimal control approach is able to

describe the aforementioned differences of human behavior in manual and shared control. For this, we conducted a study where 42 participants performed a tracking task of a given trajectory, with and without haptic assistance. As mentioned before, similar studies concerning human behavior in shared control have been published (see e.g. [2], [22]). However, the study of paper is the first to be performed from a control-theoretical perspective.

The rest of the paper is organized as follows. Section II will show our shared control modeling approach. In Section III, we describe the method we employ for identification of the cost function. Afterwards, we describe in Section IV the details of the conducted study and discuss the results in Section V. Finally, conclusions are drawn and given in Section VI.

II. HUMAN BEHAVIOR IN SHARED CONTROL TASKS

In this paper, we consider a dynamic system which is controlled by a human and an automatic controller simultaneously. Fig. 1 shows the resulting shared control structure. Note the feedback in the controls which represent the haptic interaction between both cooperation partners. The dynamics of the system are described by a discrete time equation

$$\mathbf{x}^{[k+1]} = \mathbf{A}^{[k]}\mathbf{x}^{[k]} + \mathbf{B}_H^{[k]}\mathbf{u}_H^{[k]} + \mathbf{B}_A^{[k]}\mathbf{u}_A^{[k]} \quad (1a)$$

$$\mathbf{x}^{[0]} = \mathbf{x}_0. \quad (1b)$$

where \mathbf{x}_0 denotes the known system initial state. This means, both the human and the automation have an influence on the state variables $\mathbf{x}^{[k]} \in \mathbb{R}^n$ by means of their own control variables $\mathbf{u}_H^{[k]} \in \mathbb{R}^{m_H}$ and $\mathbf{u}_A^{[k]} \in \mathbb{R}^{m_A}$, respectively. The case $\mathbf{u}_A^{[k]} = 0$ for all time steps k corresponds to a manual control, i.e. without any assistance from the automation.

In this paper, we will analyze human behavior by collecting the state and control trajectories which arise during a certain time interval. The observed trajectories are denoted by

$$\underline{\mathbf{x}} = \left[(\mathbf{x}^{[1]})^\top \quad \dots \quad (\mathbf{x}^{[K]})^\top \right]^\top \in \mathbb{R}^{nK} \quad (2)$$

and

$$\underline{\mathbf{u}}_H = \left[(\mathbf{u}_H^{[1]})^\top \quad \dots \quad (\mathbf{u}_H^{[K]})^\top \right]^\top \in \mathbb{R}^{m_H K} \quad (3)$$

for K time steps. Likewise, in a shared control scenario, we define the measured support from the automation over a time interval as

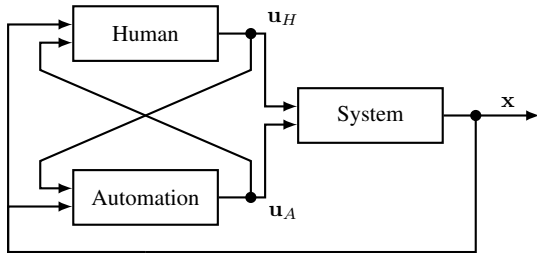


Fig. 1. Shared control of a dynamic system between a human and an automation

$$\underline{\mathbf{u}}_A = \left[(\mathbf{u}_A^{[1]})^\top \quad \dots \quad (\mathbf{u}_A^{[K]})^\top \right]^\top \in \mathbb{R}^{m_A K}. \quad (4)$$

We follow an optimal control approach for modeling human behavior and thus assume the control and state sequence in (2) and (3) to arise from the minimization of a cost function. This means the human determines a control strategy to minimize the individual cost function $J(\underline{\mathbf{x}}, \underline{\mathbf{u}}_H)$. The optimal values are given by

$$\underline{\mathbf{u}}_H^* = \arg \min_{\underline{\mathbf{u}}_H} J(\underline{\mathbf{x}}, \underline{\mathbf{u}}_H). \quad (5)$$

This dynamic optimization problem is solved with respect to (1). The trajectories $\underline{\mathbf{x}}^*$ follow directly from the control strategy $\underline{\mathbf{u}}_H^*$ and the initial value \mathbf{x}_0 .

Within the frame of this paper, we assume the cost function to have the quadratic structure

$$J_H = \sum_{k=1}^K e^{[k]^\top} \mathbf{Q}_H e^{[k]} + \mathbf{u}_H^{[k]^\top} \mathbf{R}_H \mathbf{u}_H^{[k]}, \quad (6)$$

with $e^{[k]} = \mathbf{x}^{[k]} - \mathbf{x}_{\text{ref}}^{[k]}$ and the parametrization being given by the matrices $\mathbf{Q}_H \in \mathbb{R}^{n \times n}$ and $\mathbf{R}_H \in \mathbb{R}^{m_H \times m_H}$. We denote the cost function parameters of the human as $\boldsymbol{\theta}_H$ which in this case is a vector including all elements of \mathbf{Q}_H and \mathbf{R}_H .

For the analysis of human behavior in a manual and shared control task, the individual parameters $\boldsymbol{\theta}_H$ have to be determined by an identification method. The identification problem is, given measured state and control trajectories $\tilde{\underline{\mathbf{x}}}$, $\tilde{\underline{\mathbf{u}}}_H$ (and $\tilde{\underline{\mathbf{u}}}_A$ in the shared control case), determine parameters $\boldsymbol{\theta}_H$ such that (5) holds. Furthermore, we assume knowledge of the system dynamics (1a) and the initial state value (1b). In this paper, we use a maximum entropy based inverse reinforcement learning approach which we will describe in the following section.

III. IDENTIFICATION METHOD

A. Continuous Maximum Entropy Inverse Reinforcement Learning

For identification of $\boldsymbol{\theta}_H$, we use maximum entropy inverse reinforcement learning, an approach first introduced by [23] for finite and discrete valued states and controls. Using the principle of maximum entropy aids in resolving the ambiguity and ill-posedness nature of inverse optimization problems and leads to the least biased estimate possible on the given information [24]. In this framework, the observed trajectories are assumed to be sampled by a density $p(\zeta)$, $\zeta = \{\underline{\mathbf{x}}, \underline{\mathbf{u}}\}$. We denote d samples of observed human trajectories as $\zeta_{H_l} = \{\tilde{\underline{\mathbf{x}}}_l, \tilde{\underline{\mathbf{u}}}_{H_l}\}$, $l \in \{1, \dots, d\}$.

In order to describe human behavior, continuous-valued states and controls need to be considered. This leads to an uncountable infinite set of feasible trajectories. Maximizing differential entropy with the constraint that the expert's unparametrized costs are matched leads to a probability distribution (see [23] for a derivation in the discrete-valued case)

$$p(\zeta_{H_l}) = \frac{e^{-J(\zeta_{H_l})}}{\int_{-\infty}^{\infty} e^{-J(\zeta_H)} d\tilde{\zeta}_H}. \quad (7)$$

The integral is over all possible trajectories considering (1).

The expert trajectories ζ_{H_l} are uniquely defined by the initial state $\mathbf{x}^{[0]}$ and the control strategies \mathbf{u}_H and \mathbf{u}_A due to deterministic system dynamics. Therefore, $p(\zeta_{H_l}) = p(\mathbf{u}_{H_l} | \mathbf{x}^{[0]}, \mathbf{u}_{A_l}, \boldsymbol{\theta}_H)$. Following the ideas of [25], the quadratic structure of the cost function (6) allows to rewrite the distribution as

$$p(\mathbf{u}_{H_l} | \mathbf{x}^{[0]}, \mathbf{u}_{A_l}, \boldsymbol{\theta}_H) = \frac{e^{-J(\mathbf{u}_{H_l} | \mathbf{x}^{[0]}, \boldsymbol{\theta}_H)}}{\int_{-\infty}^{\infty} e^{-J(\tilde{\mathbf{u}}_H | \mathbf{x}^{[0]}, \boldsymbol{\theta}_H)} d\tilde{\mathbf{u}}_H} \quad (8)$$

$$= e^{(-\frac{1}{2} \mathbf{g}_{H_l}^\top \mathbf{H}_{H_l}^{-1} \mathbf{g}_{H_l})} |\mathbf{H}_{H_l}|^{\frac{1}{2}} (2\pi)^{-\frac{n_T}{2}},$$

where

$$\mathbf{g}_{H_l} = \left. \frac{\partial J}{\partial \mathbf{u}} \right|_{\mathbf{u}_{H_l}} \in \mathbb{R}^{m_H K} \quad (9)$$

and

$$\mathbf{H}_{H_l} = \left. \frac{\partial^2 J}{\partial \mathbf{u}^2} \right|_{\mathbf{u}_{H_l}} \in \mathbb{R}^{m_H K \times m_H K}. \quad (10)$$

These represent the first and second derivative of the cost function with respect to the control value sequence \mathbf{u}_{H_l} .

B. Approach for Affine System Dynamics

In [25], calculations are given for the gradient \mathbf{g} and hessian \mathbf{H} for linear discrete-time system dynamics. Our shared control model involves an affine system (see (1)) from the point of view of the human, since \mathbf{u}_A is an external signal from the automation. Thus, we introduce new calculations such that the affine term is considered in the solution of the identification problem. For this, we note that \mathbf{x} , \mathbf{u}_H and \mathbf{u}_A as defined in (2)–(4) are related through the extended system equation

$$\mathbf{x} = \mathbf{A}\mathbf{x}^{[0]} + \mathbf{B}_H \mathbf{u}_H + \mathbf{B}_A \mathbf{u}_A \quad (11)$$

where \mathbf{A} , \mathbf{B}_H are defined as

$$\mathbf{A} = [\mathbf{A}^1 \quad \mathbf{A}^2 \quad \dots \quad \mathbf{A}^K]^\top,$$

$$\mathbf{B}_H = \begin{bmatrix} \mathbf{B}_H & \mathbf{0} & \dots & \mathbf{0} \\ \mathbf{A}^1 \mathbf{B}_H & \mathbf{B}_H & & \vdots \\ \vdots & \vdots & \ddots & \mathbf{0} \\ \mathbf{A}^{K-1} \mathbf{B}_H & \mathbf{A}^{K-2} \mathbf{B}_H & \dots & \mathbf{B}_H \end{bmatrix}. \quad (12)$$

The matrix \mathbf{B}_A is defined analogously to \mathbf{B}_H .

With the previous definitions, the cost function of the human (6) may be rewritten as

$$J_H = (\mathbf{x} - \mathbf{x}_{\text{ref}})^\top \mathbf{Q}_H (\mathbf{x} - \mathbf{x}_{\text{ref}}) + \mathbf{u}_H^\top \mathbf{R}_H \mathbf{u}_H \quad (13)$$

where \mathbf{x} is given by (11) and the aggregated matrix \mathbf{Q}_H is defined as

$$\mathbf{Q}_H = \begin{bmatrix} \mathbf{Q}_H & \mathbf{0} & \dots & \mathbf{0} \\ \mathbf{0} & \mathbf{Q}_H & \dots & \vdots \\ \vdots & \vdots & \ddots & \mathbf{0} \\ \mathbf{0} & \dots & \mathbf{0} & \mathbf{Q}_H \end{bmatrix}. \quad (14)$$



Fig. 2. Steering wheel and visualization monitor used for the experiment

The matrix \mathbf{R}_H is defined analogously to \mathbf{Q}_H . Now the cost function (13) can be derived with respect to \mathbf{u}_H , which yields for the gradient

$$\mathbf{g}_{H_l} = 2\mathbf{B}_H^\top \mathbf{Q}_H \left(\underbrace{\mathbf{A}\mathbf{x}^{[0]} + \mathbf{B}_H \mathbf{u}_H + \mathbf{B}_A \mathbf{u}_A}_{\mathbf{x}} - \mathbf{x}_{\text{ref}} \right) + 2\mathbf{R}_H \mathbf{u}_H \quad (15)$$

and for the hessian

$$\mathbf{H}_{H_l} = 2\mathbf{B}_H^\top \mathbf{Q}_H \mathbf{B}_H + 2\mathbf{R}_H. \quad (16)$$

With these derivatives, the approximation for the probability distribution in (8) can be calculated. Let d observed expert demonstrations be given by $\mathcal{D} = \{\zeta_{H_1}, \dots, \zeta_{H_d}\}$ with $\zeta_{H_l} = \{\tilde{\mathbf{x}}_{H_l}, \tilde{\mathbf{u}}_{H_l}\}$, $l = 1, \dots, d$. Now we determine

$$\hat{\boldsymbol{\theta}}_H = \arg \max_{\boldsymbol{\theta}_H} \prod_{l=1}^d p(\zeta_{H_l}) = \arg \max_{\boldsymbol{\theta}_H} \sum_{l=1}^d \ln(p(\zeta_{H_l})), \quad (17)$$

where $\hat{\boldsymbol{\theta}}_H$ is an estimate for the parameters of the human's cost function. This is a parameter optimization problem which can be solved using standard algorithms.

IV. EXPERIMENTAL SETUP

We conducted a study in order to evaluate human behavior in manual and shared control tasks. The control task consisted in following a reference trajectory by means of a steering wheel. The human shared control with an automatic controller which gave haptic assistance in the mentioned task.

A. Experimental Framework

We used an experimental framework consisting of three main components: an active steering wheel, a monitor with a visualization window and a real-time environment which also realizes the communication between all components. The measurements of the steering wheel angle are done by an incremental encoder of 40000 increments per full rotation at a sampling frequency of $f_s = 100$ Hz. Fig. 2 shows the components of the experiment.

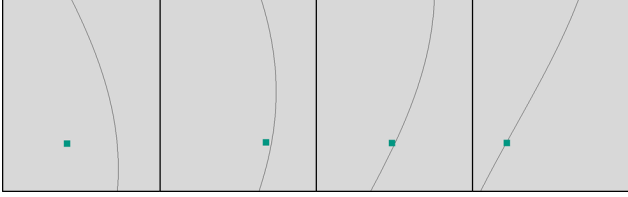


Fig. 3. Visualization of the control task. The picture sequence is from left to right.

TABLE I
STEERING WHEEL PARAMETERS

Parameter	Value		Description
Θ_L	0.04	kg m ²	Steering wheel rotational inertia
c	1.146	Nm/rad	Spring constant
d	0.286	Nm · s/rad	Damping constant

B. Tracking Task

Fig. 3 shows a sequence of screen captures from the experiment visualization. The participants can control the horizontal position of the marker (square) by means of the steering wheel in order to follow a reference trajectory which passes downwards through the visualization window. A point of the reference signal crosses the entire visualization window in 2 seconds. The vertical position of the marker is fixed at a height of 25%.

C. System Dynamics and Human Cost Function

The dynamics of the steering wheel which is controlled by the human and the automation is given by

$$\dot{\mathbf{x}} = \begin{bmatrix} 0 & 1 \\ -\frac{c}{\Theta_L} & -\frac{d}{\Theta_L} \end{bmatrix} \mathbf{x} + \begin{bmatrix} 0 \\ \frac{1}{\Theta_L} \end{bmatrix} u_H + \begin{bmatrix} 0 \\ \frac{1}{\Theta_L} \end{bmatrix} u_A, \quad (18)$$

where $\mathbf{x} = [\varphi \ \dot{\varphi}]^\top$ and $u_H = M_H$ and $u_A = M_A$ the steering torque applied by the human and the automatic controller, respectively. The parameters of the system are given in Table I. This system was discretized using a sample time of $T_s = 1/f_s = 0.01$ s in order to get the discrete-time representation given in (1).

The cost function is given by (6) and is parameterized by a vector $\boldsymbol{\theta}_H = [q_{11} \ q_{22} \ R] \in \mathbb{R}^3$. We chose to neglect the parameters q_{12} and q_{21} by setting them to zero since these represent angle-velocity mixed terms in the cost function which are neither meaningful nor interpretable. This is a common procedure in optimal control theory [26]. The state reference is given by $\mathbf{x}_{\text{ref}}^{[k]} = [x_{1,\text{ref}}^{[k]} \ x_{2,\text{ref}}^{[k]}]^\top$, where $x_{1,\text{ref}}^{[k]}$ is the reference trajectory for the steering angle which is visible in the monitor and $x_{2,\text{ref}}^{[k]} = 0$ for all time steps k , since the human does not follow a particular velocity reference signal.

D. Assistance System

The haptic assistance was generated by a model predictive controller (MPC) which calculates the control values based on the dynamic optimization problem

$$\min_{\mathbf{u}_A} J_A = \sum_{k=1}^{N_P} e^{[k]\top} \mathbf{Q}_H e^{[k]} + \mathbf{u}_A^{[k]\top} \mathbf{R}_H \mathbf{u}_A^{[k]} \quad (19)$$

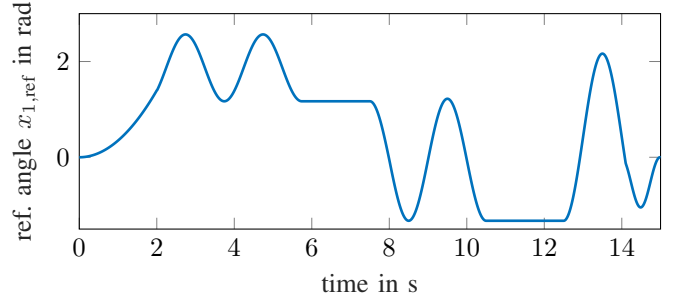


Fig. 4. Reference trajectory used for cost function parameter identification

with respect to the discretized system (18) with $u_H = 0$. This means the assistance system behaves the same for all test subjects. The dynamic optimization problem is solved for a prediction horizon of the length $N_P = 50$ with a sample rate of $T_C = 0.02$ s. Note that the cost function was given the same structure as the cost function of the human (6). We chose the parameter values $\boldsymbol{\theta}_A = [5 \ 0 \ 1]^\top$ which lead to a slight assistance level. This means that the haptic guidance is not able to track the given trajectory perfectly on its own.

E. Data Acquisition

In order to apply the identification algorithm, a demonstration ζ_H which consists of all states and the control values is needed. As mentioned in Section IV-A, only a sensor for measuring the steering angle x_1 is available. Therefore, the steering angle velocity x_2 and the steering torque u_H were calculated offline by means of the system dynamics equation given in (18). In addition, \mathbf{u}_A is needed for identification in the shared control scenario. This data can be retrieved and stored directly from the MPC output.

F. Experimental Protocol

We conducted a study with 42 subjects (age 23.4 ± 5.54). They did not have prior knowledge of the research subject and also never participated in a study concerning the experimental design described previously. The subjects were told to move the steering wheel in such a way that the marker matches the reference trajectory. There were two test runs:

- 1) A 4-minute test run without any haptic assistance (manual control)
- 2) A 4-minute test run with haptic assistance (shared control)

The order was selected randomly for each subject.

For identification of the individual cost function parameters, only one part of the whole trajectory was considered. The first minutes of each run were included as a time to become familiar with the experimental design and the dynamics of the steering wheel. The trajectory piece used for our analysis started after 3 minutes and 30 seconds and is depicted in Fig. 4. This reference trajectory was the same for all subjects, in both the manual and shared control scenario. After this trajectory, there was another following trajectory piece of 15 s which was also not considered in the evaluation. The subjects were unaware of all of these details.

We denote the human demonstrations corresponding to Fig. 4 in the manual control task as $\zeta_{H,MC}^{(i)}$ and in the shared control task as $\zeta_{H,SC}^{(i)}$ for each test person i . These were used to determine cost function parameters by solving (17) (with $l = 1$), for which we applied a sequential quadratic programming method. This leads to cost function parameters $\theta_{H,MC}^{(i)}$ and $\theta_{H,SC}^{(i)}$, $i \in \{1, \dots, 42\}$ corresponding to the manual control task and shared control scenario, respectively.

G. Hypothesis and Evaluation Method

The hypothesis we state for the study is the following:

Hypothesis 1 [H_1]

If the human completes a control task in a haptic shared control scenario, then a considerable change in the specific cost function parameters θ_H can be detected with respect to a manual control task.

In order to evaluate this hypothesis, we use the identified cost function parameters $\theta_{H,MC}^{(i)}$ and $\theta_{H,SC}^{(i)}$ of each subject. As we are comparing two different samples, we chose the Wilcoxon matched-pairs signed-rank test [27] for evaluation. With this test, we examine whether the two samples (manual and shared control) stem from two different statistical populations.

V. RESULTS AND DISCUSSION

A. Results

Beforehand, we normalized the cost function parameters of each subject with respect to θ_3 in order to ensure comparability. It is worth mentioning that this does not affect the results since a cost function $J(\cdot)$ yields the same optimal solution as $cJ(\cdot)$, $c \in \mathbb{R}^+$. The parameter θ_2 (which weights the velocity) was always equal to zero for all test subjects. Fig. 5 shows a histogram with the identified θ_1 in the manual control and the shared control task. A difference in the parameter distribution can be discerned. This is confirmed by the statistical test, where the null hypothesis was rejected with a significance level of $\alpha = 0.1\%$ and the amount of pairs $N = 42$. The test yielded a rank sum of $3 < P(0.1; 42) = 195$. The null hypothesis states that the samples come from the same statistical population. This means that hypothesis H_1 is accepted.

In [28], it was shown that maximum entropy based inverse reinforcement learning techniques are suitable for describing individual human behavior. Thus, we show here exemplarily only the results of test subject 3. The measured trajectories $\zeta_{H,MC}$ are compared with the trajectories generated by the cost function parameters $\theta_{H,MC}$ and $\theta_{H,SC}$. The latter two trajectories can be generated by solving a forward dynamic optimization problem using the aforementioned parameters. All trajectories are depicted in Fig. 6.

B. Discussion

In Fig. 6, it stands out that the state trajectories x_1 and x_2 are very similar in all cases, which means that the subject was able to track the reference trajectory in an acceptable way regardless of any haptic support. However, we can recognize

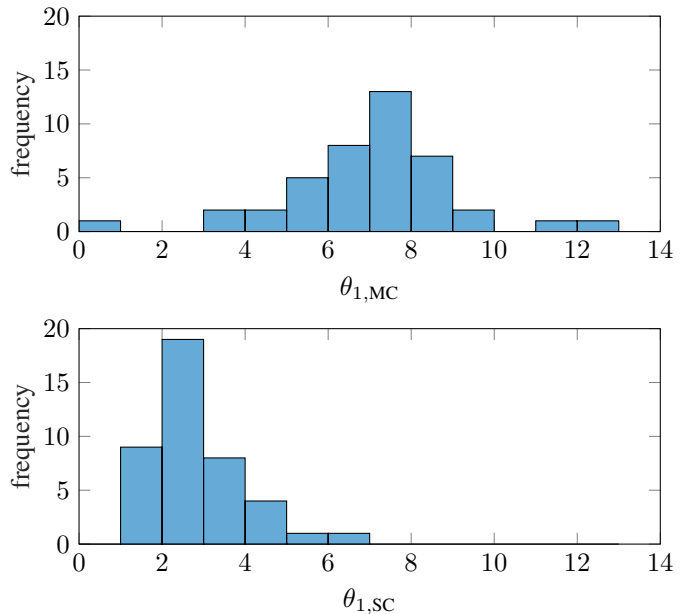


Fig. 5. Histogram of identified parameters $\theta_1 = q_{11}$ in the shared control (SC) and in the manual control (MC) task.

that the applied steering torque is significantly different when regarding the shared control scenario. We further discern that the human behavior models based on the cost function parameters $\theta_{H,MC}$ and $\theta_{H,SC}$ are both able to explain the state and control trajectories of the manual control task and the shared control task, respectively. The cost function with $\theta_{H,MC}$ can approximate the state trajectories adequately in both scenarios and hence, this initially suggests that both cost functions are acceptable as a human behavior model in shared control. However, the cost function with the parameters $\theta_{H,MC}$ cannot explain the new human steering torque which arised in the shared control scenario. It is important to recall that the prediction of human control input is crucial to shared control. Ignoring differences in the control input implies strong disagreements between both partners, leading to reduced user acceptance and even stability issues. As a consequence, the results indicate that a suitable controller design for shared control should be based upon an identification of the human cost function in a shared control task, hence considering the interaction with the machine.

VI. CONCLUSION

This paper analyzed and compared human behavior in a control task with and without haptic assistance, i.e. in a manual control mode and in a shared control scenario. We presented an optimal control modeling approach, where human behavior is described by a parametrized cost function and applied an inverse optimization technique to identify individual parameters. Furthermore, we hypothesized that the identified cost function which describes human behavior is different if the human is in a shared control scenario. The test data confirmed our hypothesis and showed the suitability of the presented optimal control approach to describe human behavior in both manual

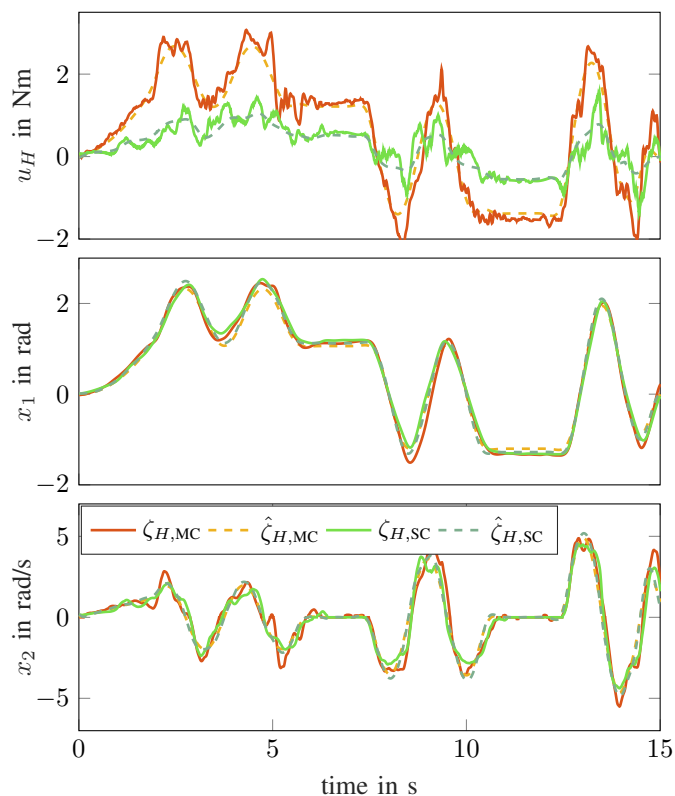


Fig. 6. Comparison of measured trajectories in the manual control task (red) and in the shared control task (green) performed by test subject 3 with the trajectories generated by the human optimal control model with the two different parametrizations (dashed).

and shared control. In a broader sense, the results of this paper emphasize the importance of including the interaction with the machine when determining a human behavior model to be applied in shared control. For example, within the optimal control approach, the cost function identified out of measured data in a manual control task has been shown to yield trajectories which do not explain observed data in a shared control scenario adequately. In particular, major deviations can be recognized in the steering torque trajectories which is a crucial quantity due to the haptic interaction between human and machine.

REFERENCES

- [1] L. Bainbridge, "Ironies of automation," *Automatica*, vol. 19, no. 6, pp. 775–779, 1983.
- [2] M. Mulder, D. A. Abbink, and E. R. Boer, "Sharing Control With Haptics: Seamless Driver Support From Manual to Automatic Control," *Human Factors*, vol. 54, no. 5, pp. 786–798, 2012.
- [3] M. Mulder, S. Kitazaki, S. Hijikata, M. Mulder, M. M. v. Paassen, and E. R. Boer, "Reaction-time task during car-following with an active gas pedal," in *IEEE International Conference on Systems, Man and Cybernetics*, vol. 3, 2004, pp. 2465–2470 vol.3.
- [4] H. Boessenkool, D. A. Abbink, C. J. M. Heemskerk, F. C. T. v. d. Helm, and J. G. W. Wildenbeest, "A Task-Specific Analysis of the Benefit of Haptic Shared Control During Telemanipulation," *IEEE Transactions on Haptics*, vol. 6, no. 1, pp. 2–12, 2013.
- [5] Y. Tanaka, "Robot-Aided Rehabilitation Methodology for Enhancing Movement Smoothness by Using a Human Trajectory Generation Model With Task-Related Constraints," *Journal of Human-Robot Interaction*, vol. 4, no. 3, p. 101, 2015.
- [6] K. Shamaei, Y. Che, A. Murali, S. Sen, S. Patil, K. Goldberg, and A. M. Okamura, "A paced shared-control teleoperated architecture for supervised automation of multilateral surgical tasks," in *IEEE International Conference on Intelligent Robots and Systems (IROS)*, 2015, pp. 1434–1439.
- [7] D. Abbink, M. Mulder, and E. Boer, "Haptic shared control: Smoothly shifting control authority?" *Cognition, Technology & Work*, vol. 14, no. 1, 2012.
- [8] J. Smisek, E. Sunil, M. M. v. Paassen, D. A. Abbink, and M. Mulder, "Neuromuscular-System-Based Tuning of a Haptic Shared Control Interface for UAV Teleoperation," *IEEE Transactions on Human-Machine Systems*, vol. 47, no. 4, pp. 449–461, 2017.
- [9] F. Mars and P. Chevrel, "Modelling human control of steering for the design of advanced driver assistance systems," *Annual Reviews in Control*, vol. 44, pp. 292–302, 2017.
- [10] D. Abbink, D. Cleij, M. Mulder, and M. van Paassen, "The importance of including knowledge of neuromuscular behaviour in haptic shared control," in *IEEE International Conference on Systems, Man, and Cybernetics (SMC)*, 2012, pp. 3350–3355.
- [11] M. Flad, J. Otten, S. Schwab, and S. Hohmann, "Necessary and sufficient conditions for the design of cooperative shared control," in *IEEE International Conference on Systems, Man and Cybernetics (SMC)*, 2014, pp. 1253–1259.
- [12] B. Berret, E. Chiovetto, F. Nori, and T. Pozzo, "Evidence for Composite Cost Functions in Arm Movement Planning: An Inverse Optimal Control Approach," *PLoS Computational Biology*, vol. 7, no. 10, 2011.
- [13] M. C. Priess, R. Conway, J. Choi, J. M. J. Popovich, and C. Radcliffe, "Solutions to the inverse lqr problem with application to biological systems analysis," *IEEE Transactions on Control Systems Technology*, vol. 23, no. 2, pp. 770–777, 2015.
- [14] E. Todorov, "Optimality principles in sensorimotor control," *Nature Neuroscience*, vol. 7, no. 9, pp. 907–915, 2004.
- [15] W. Li, E. Todorov, and D. Liu, "Inverse optimality design for biological movement systems," *IFAC World Congress*, 2011.
- [16] S. Scott, "Optimal feedback control and the neural basis of volitional motor control," *Nature Reviews Neuroscience*, vol. 5, no. 7, pp. 532–546, 2004.
- [17] K. Mombaur, A. Truong, and J. Laumond, "From human to humanoid locomotion inverse optimal control approach," *Autonomous Robots*, vol. 28, no. 3, pp. 369–383, 2010.
- [18] M. Johnson, N. Aghasadeghi, and T. Bretl, "Inverse optimal control for deterministic continuous-time nonlinear systems," in *IEEE 52nd Annual Conference on Decision and Control (CDC)*, 2013, pp. 2906–2913.
- [19] P. Abbeel and A. Y. Ng, "Apprenticeship learning via inverse reinforcement learning," in *Proceedings of the twenty-first international conference on Machine learning*. ACM Press, 2004, p. 1.
- [20] S. Miossec and A. Kheddar, "Human motion in cooperative tasks: Moving object case study," in *IEEE International Conference on Robotics and Biomimetics (ROBIO)*, 2009, pp. 1509–1514.
- [21] D. Feth, R. Groten, A. Peer, and M. Buss, "Control-theoretic model of haptic human-human interaction in a pursuit tracking task," in *18th IEEE International Symposium on Robot and Human Interactive Communication*, 2009, pp. 1106–1111.
- [22] M. Mulder, D. A. Abbink, and E. R. Boer, "The effect of haptic guidance on curve negotiation behavior of young experienced drivers," in *IEEE International Conference on Systems, Man and Cybernetics (SMC)*, 2008, pp. 804–809.
- [23] B. Ziebart, A. Maas, J. Bagnell, and A. Dey, "Maximum entropy inverse reinforcement learning," in *Proceedings of the 23rd National Conference on Artificial Intelligence (AAAI)*, 2008, pp. 1433–1438.
- [24] E. Jaynes, "Information theory and statistical mechanics," *Physical Review*, vol. 106, no. 4, pp. 620–630, 1957.
- [25] S. Levine and V. Koltun, "Continuous inverse optimal control with locally optimal examples," in *Proceedings of the 29th International Conference on Machine Learning (ICML)*, 2012, pp. 41–48.
- [26] D. E. Kirk, *Optimal control theory: an introduction*. Prentice-Hall, 2004.
- [27] S. Siegel and N. J. Castellan, *Nonparametric Statistics for the Behavioral Sciences*, 2nd ed. MacGraw-Hill, 1988.
- [28] J. Inga, F. Köpf, M. Flad, and S. Hohmann, "Individual human behavior identification using an inverse reinforcement learning method," in *IEEE International Conference on Systems, Man, and Cybernetics (SMC)*, 2017, pp. 99–104.